Synergistic effect of radial electric field and magnetic shear on ion temperature gradient mode

Qien Jing[1], Yuehao Ma[2], Zhihong Lin[3], Huishan Cai[2,*]

[1]University of Science and Technology of China, Hefei 230026, China
[2]CAS Key Laboratory of Frontier in Controlled Nuclear Fusion, and School of Nuclear Sciences and Technology, University of Science and Technology of China
[3]Department of Physics and Astronomy, University of California, Irvine, CA 92697, United States of America

E-mail: hscai@mail.ustc.edu.cn

September 2024

Abstract. Based on the Gyrokinetic Toroidal Code (GTC), the synergistic effect of the radial electric field (E_r) shear and the magnetic shear on ion temperature gradient (ITG) instabilities of an Experimental Advanced Superconducting Tokamak (EAST) discharge (#93890) is studied. It is found that the synergistic effect of the magnetic shear and the E_r shear is significant in stabilizing ITG mode. Whether the E_r shear plays a stable role or destabilizing role depends on both the relative direction of the E_r shear and the magnetic shear, and the amplitude of the E_r shear. Specifically, the E_r shear with negative shearing rate has more efficient stabilizing effect under the weakly reverse magnetic shear. Based on the experimental E_r profile, it is shown that the global effect of E_r on the stabilization of micro-instabilities needs to be considered. The E_r with the $\omega_s = 0$ at the inner side of the ITG mode shows a better stabilizing effect, because of the synergistic effect of negative shearing rate and weakly reverse magnetic shear at the ITG mode location. The results indicate that the positive feedback between the formation of ITB and the formation of E_r well with an optimized magnetic shear might be the key to the long-time existence of ITB.

Keywords: radial electric field, ion temperature gradient, magnetic shear, EAST plasma

1. Introduction

In a tokamak, ion temperature gradient (ITG) micro-instabilities dominate the ion heat transport channel, could be unfavorable to plasma confinement. Inside the internal transport barrier (ITB), the gradient of temperature or density is high, due to the reduction of anomalous transport caused by turbulence. Most theoretical models for ITB formation ultimately rely on the stabilization of micro-instability induced transport by the magnetic shear and the sheared $E \times B$ flows [1, 2, 3]. Previous studies have shown that the E_r shear plays an important role in tokamak because it has a stabilizing effect on microturbulence and reduces the turbulent transport level to improve the plasma confinement [4, 5, 6, 7]. It has been experimentally confirmed on tokamak that increase in shear rate ($\omega_{E\times B}$), which is normally used for describing the strength of the sheared flow, would stabilize ITG instabilities and promote the formation of ITB [8]. On the other hand, the appropriate magnetic shear can stabilize the instability and be in favor of the formation of ITB [1, 9]. Therefore, understanding the synergistic effect of the E_r shear and the magnetic shear on stabilizing ITG instabilities is significant for improving the operational stability of fusion plasma. Previous simulation studies showed that E_r shear always plays a stabilizing role on ITG under different magnetic shears [4, 5], despite the effect is enhanced with increasing magnetic shear [3].

The appropriate magnetic shear and the E_r shear will both tilt the structure of the ballooning mode and reduce the growth rate of the mode [2, 3, 4]. However, the different direction of these shear effect will tilt mode structure in different direction. Therefore, the synergistic effect of the E_r shear and the magnetic shear is important because the synergistic effect determines the tilting direction of the mode structure, which might cause the E_r shear become a destabilizing effect. Based on these physical considerations, in this work, the performance of the synergistic effect of the E_r shear and the magnetic shear on ITG instabilities on EAST are studied using the gyrokinetic toroidal code (GTC).

The remainder of this paper is organized as follows. The physical model and simulation setup are described in section 2. The stabilizing performance of synergistic effect of the E_r shear and magnetic shear on microturbulence is discussed in section 3. The further research using the experimental E_r profile is discussed in section 4. Section 5 gives a summary of the study.

2. Physical model and simulation setup

This study focuses on the synergistic effect of equilibrium radial electric fields and magnetic shear on electrostatic drift wave turbulence. The detail of the gyrokinetic models utilized in the GTC code have been previously discussed in [4, 10, 11]. To account for the influence of the equilibrium radial electric field E_r, the electrostatic potential $\phi = \delta\phi + \phi_{eq}$ is incorporated into the gyrokinetic equations [4], where ϕ_{eq} is the equilibrium electrostatic potential[2].

The equilibrium electric field will impact the ITG plasma in two important ways. Firstly, the rigid rotation caused by $E \times B$ drift will change the frequency of the ITG mode, i.e. doppler shift $\Omega_E = -n\mathrm{d}\phi_{eq}/\mathrm{d}\psi$ [12]. Secondly, the sheared flow caused by E_r will reduce the linear growth rate of ITG mode and affect the saturation amplitude.

In our study, the simulations of electrostatic turbulence are conducted using experimental data from EAST tokamak discharge (#93890) at 5000ms, where both the plasma profile and magnetic geometry have previously been discussed in [11, 13]. As shown in Fig. 1, both the electron and ion densities, as well as temperatures, exhibit an internal transport barrier (ITB) in the presence of weakly negative magnetic shear. Our simulation domain is delineated in the radial normalized range $r/a \in [0.10, 0.52]$, as indicated by the gray dashed line in Fig. 1. Dirichlet boundary conditions are applied due to the negligible turbulence perturbations near the boundary. The other simulation parameters used for convergent physical run are 150 radial grids, 32 toroidal grids and 600 poloidal grids in the simulation domain. The time step is $\Delta t = 0.005 R_0/C_s$ (where C_s is the sound speed on magnetic axis).

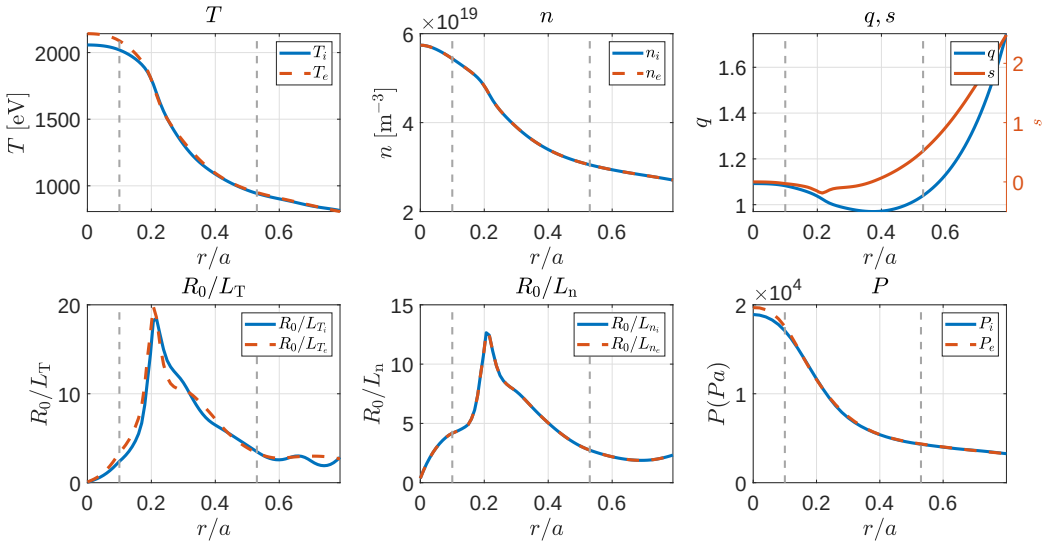

Figure 1: Plasma radial profile in EAST discharge #93890 at 5000 ms, and the simulation region is noticed by gray dashed line. The top row, from left to right, shows temperatures (T), density (n) for ions (subscript i) and electrons (subscript e), safety factor (q) and magnetic shear (s) respectively. The bottom row, from left to right, shows the inverse temperature length scales (R_0/L_T), the inverse density length scale (R_0/L_n), pressure for ions and electrons respectively.

3. Radial electric field shear effects on ITG

3.1. ITG mode dispersion relation and frequency Doppler shift caused by E_r shear

To study the performance of the synergistic effect of the E_r shear and the magnetic shear on stabilizing ITG instabilities, the dispersion relation with E_r should be verified in the physical model. The dispersion relation without E_r in the simulation domain has

been well researched previously in the report [11], showing that the peak value of the ITG linear growth rate γ is $k_\theta \rho_i \approx 1$ ($n = 25$). Now, we use a constant $\mathrm{d}\phi/\mathrm{d}\psi$ ($\omega_s = 0$) profile to verify the Doppler shift effect on ITG mode, where $\omega_s = -\frac{(R_0 B_p)^2}{B_0}\partial^2\phi_{eq}/\partial\psi^2$ is shearing rate [4]. The simulation results of the mode frequency, both without E_r and with E_r ($\omega_s = 0$), are depicted in Fig. 2a.

The simulation results with E_r ($\omega_s = 0$) agree well with the theoretical results calculated by the Doppler shifted effect [12]. Additionally, the linear growth rates without E_r and with E_r ($\omega_s = 0$) have no obvious difference, indicating the E_r with $\omega_s = 0$ has nearly no stabilizing effect on ITG mode. The Doppler shift effect of the ITG mode is similar to the results on CBC case [4].

Moreover, to verify the impact of the E_r shear on the linear growth rate of modes, we scan different toroidal numbers n under E_r with constant $\omega_s = 0, 0.1$, which is shown in Fig. 2b. The $n = 25$ mode is the most unstable mode under different constant ω_s. However, the presence of E_r shear increases the growth rate, which is different from the result where E_r shear decreases the growth rate of ITG mode [4, 5, 6]. Next, we focus on the most unstable case ($n = 25$) to study the effect of E_r shear on ITG mode.

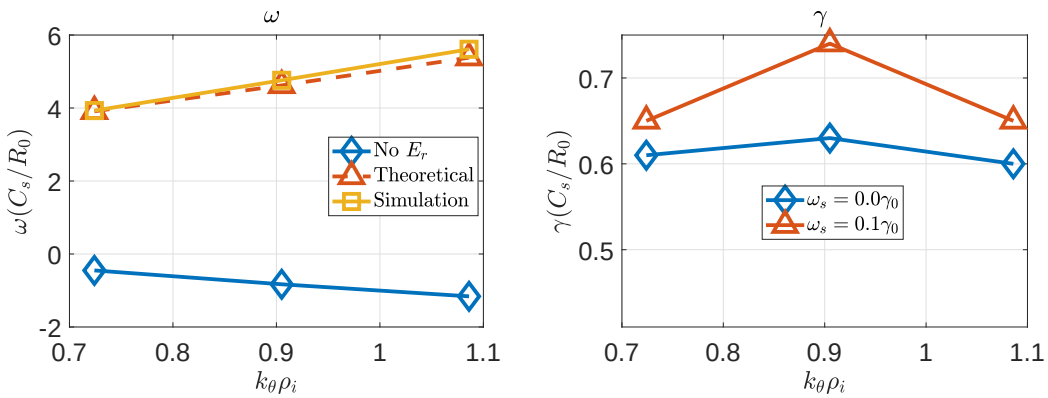

Figure 2: (a) shows the mode frequency of ITG mode are represented by the blue line (without Er), the orange line (with ω_s for E_r) and the red dashed line (theoretical results), respectively. (b) shows the linear growth rate of ITG versus poloidal wavelength $k_\theta\rho_i$ (corresponding to toroidal mode number $n = 20, 25, 30$) under constant $\omega_s/\gamma_0 = 0.0, 0.1$, where γ_0 is the growth rate without E_r. The E_r profile with constant ω_s are shown in Fig. 3a.

3.2. Stabilizing effects on ITG mode of the E_r shear

In the cases followed, the constant shearing rate ω_s is scanned. The ITG growth rate versus ω_s in simulation are shown in Fig. 3. For $\omega_s > 0$, the growth rate initially increases with ω_s. As ω_s becomes large enough, the growth rate then decreases with ω_s increasing. The peak value of the linear growth rate corresponds to $\omega_s/\gamma_0 = 0.1$. For $\omega_s < 0$, the growth rate monotonically decreases with increasing $|\omega_s|$. Specially, the effect of negative shearing rate is more effective in comparison with the effect of positive

shearing rate on ITG. These results shows that the stabilizing effect of the E_r shear depends on the sign of the shear, which is different from the result shown in previous researches [4, 5, 6]. The Fig. 4 shows mode structures of $\delta\phi$ correspond to the results shown in Fig. 3. As shown in Fig. 4c, without E_r shear ($\omega_s = 0$), the ballooning angle θ_0 [14, 15, 16] is greater than zero. With the increase of positive ω_s, the E_r tilts the ITG mode structure clockwise so that the θ_0 initially decreases to zero, which is shown in Fig. 4d, and then monotonically decreases, which is shown in Fig. 4e, 4f. With the increase of negative ω_s, the E_r tilts the ITG mode structure anticlockwise so that the θ_0 monotonically increases.

The decrease in the ITG growth rate due to the E_r shear is associated with the tilt of the ITG mode structure. The mode structure tilts itself can reduce ITG mode growth rate [5]. On the other hand, the tilt increase $|\theta_0|$, which will increase the effective k_r and reduce the linear growth rate [6, 2]. Combining this mechanism, the above results of E_r shear on ITG can be understood. In the above cases on EAST, the weakly reverse magnetic shear near the ITG location, $s = -0.13$, tilts the flute-like mode structure [3] as shown in Fig. 4c. From Fig. 4d, the E_r with positive ω_s partly cancels the tilting effect of the weakly reverse magnetic shear, causing the ITG mode growth rate initially increases with the increasing positive ω_s. When the positive ω_s is large enough, the tilting effect caused by E_r shear is dominant compared with magnetic shear as shown in Fig. 4e–4f. Consequently, the ITG mode growth rate decreases with the increasing positive ω_s. For the E_r with negative ω_s, the tilting direction of the E_r shear and the magnetic shear are same, the ITG mode growth rate monotonically decreases with increasing magnitude of negative ω_s. Therefore, the stabilize effect of the sheared flow caused by the E_r shear on EAST depends on the sign of shearing rates ω_s and the negative ω_s shear is more effective than positive ω_s shear in stabilizing the ITG mode on EAST. This is different from the CBC case, where the ballooning angle $\theta_0 \to 0$ for ITG with the magnetic shear $s \approx 0.8$ at the location of maximum ITG mode amplitude in the radial direction in the absence of electric field [4, 5]. Thus, the effects of E_r shear on ITG in the CBC case are all stabilizing. Hence, the synergistic effect of E_r and magnetic shear on ITG is important. Whether the E_r shear plays a stabilizing role or not depends on the net effect contributed from the magnetic shear and the E_r shear.

3.3. Synergistic effect of E_r shear and magnetic shear on EAST

The synergistic effect of the E_r shear and the magnetic shear on EAST is further investigated in this section. We use different q profiles to obtain different magnetic shear ($s = -0.13, 0.2, 0.4, 0.6, 0.8$ at the ITG location without E_r shear) and compare the stabilizing effects on ITG mode of the E_r shear under different magnetic shear.

The q profiles we used are shown in the Fig. 5a. The Fig. 6a shows that, without E_r, the ITG growth rate γ increases with the increasing magnetic shear within $s \in [-0.13, 0.8]$. Because the decreasing magnetic shear tilts the ITG mode streamer more strongly and decreases the ITG growth rate, which is shown in Fig. 7a–7c. This

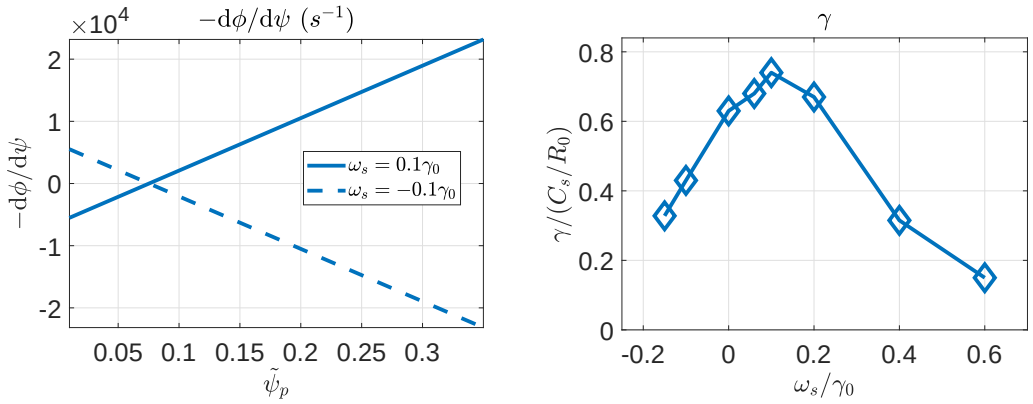

(a) (b)

Figure 3: (a) The E_r with $\omega_s/\gamma_0 = \pm 0.1$ represented by $\mathrm{d}\phi/\mathrm{d}\psi$ over normalized poloidal flux and the E_r with $\omega_s/\gamma_0 = -0.15, 0.20, 0.40, 0.60$ is generated by changing the slope of the $\mathrm{d}\phi/\mathrm{d}\psi$. Noticed that the $\omega_s = 0$ is set at the location of ITG, therefore, the doppler shift effect is not necessary to be considered. (b) Simulations results of the growth rate versus shearing rate ω_s with constant ω_s.

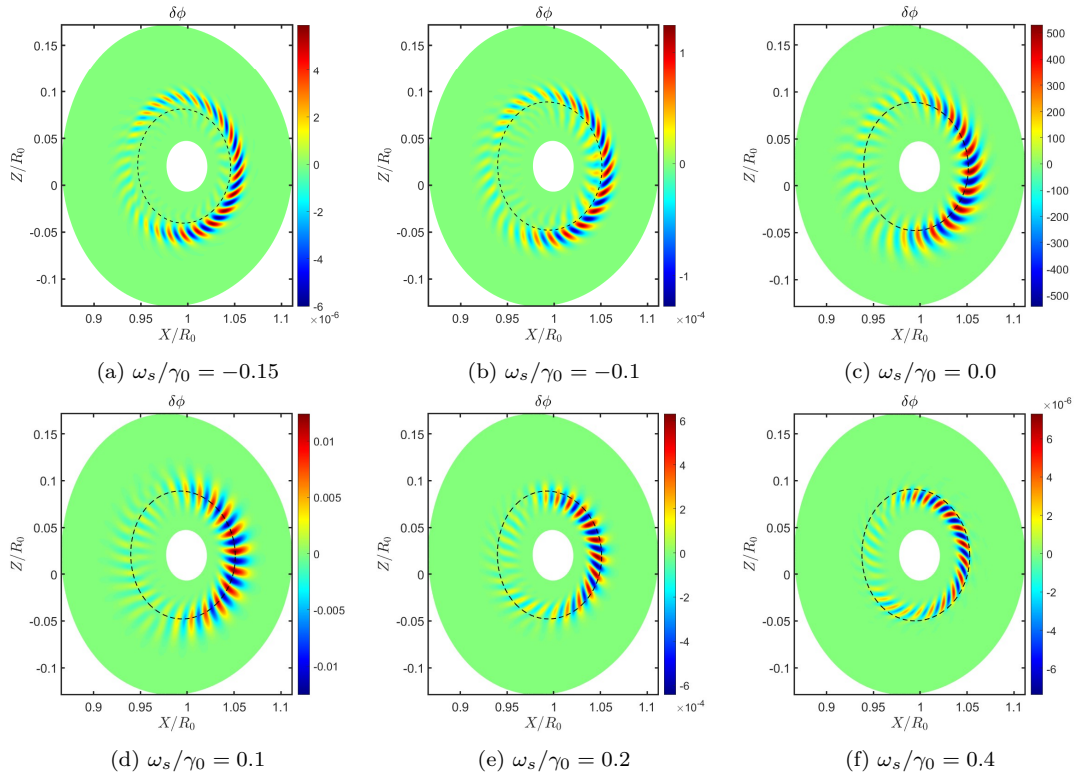

(a) $\omega_s/\gamma_0 = -0.15$ (b) $\omega_s/\gamma_0 = -0.1$ (c) $\omega_s/\gamma_0 = 0.0$

(d) $\omega_s/\gamma_0 = 0.1$ (e) $\omega_s/\gamma_0 = 0.2$ (f) $\omega_s/\gamma_0 = 0.4$

Figure 4: The poloidal mode structure of the real part of electrostatic potential with constant $\omega_s/\gamma_0 = -0.15, -0.1, 0.0, 0.1, 0.2, 0.4$. The dashed line indicates the largest η_i and $q = 1$ positions. Noted that these six mode structures are extracted from the same physical time point in same simulation conditions, the magnitudes in each figure can be directly compared.

explanation follows the mechanism we discussed in the above section. Additionally, E_r shear twists the eddy of ITG mode to good curvature direction that reduces the linear growth rate [3], which are shown in Fig. 7a–7c. Besides, the different m harmonic

coupling also contributes to the linear growth rate decrease, which is shown in Fig. 7d–7f.

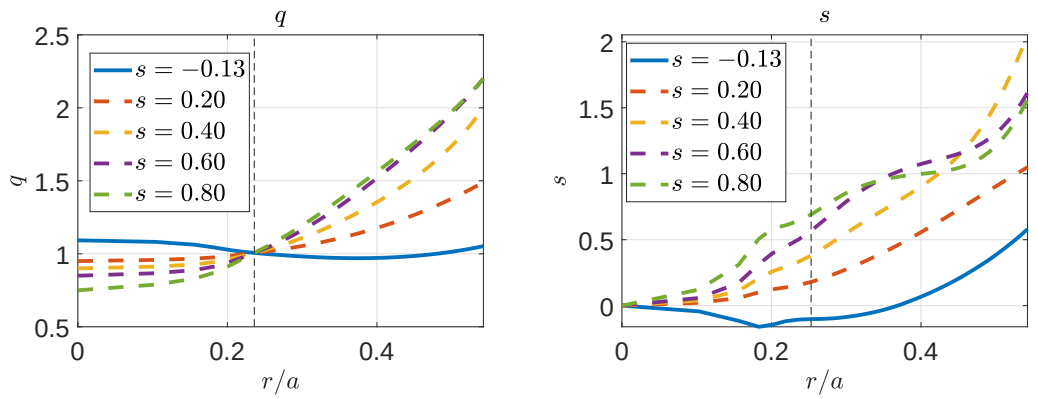

(a) (b)

Figure 5: (a) The q profiles we used to create different s. (b) Profiles of magnetic shear (s). Noticed that the value of s in legend corresponds the value at the ITG location which is indicated with gray dashed line.

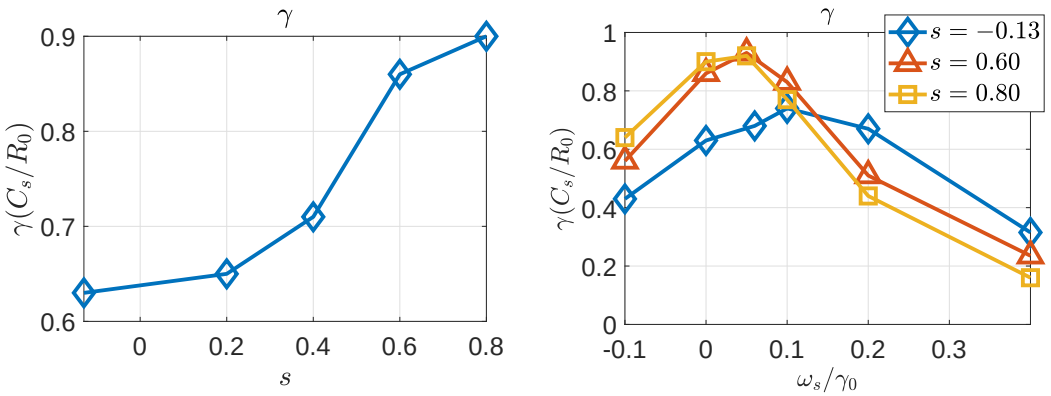

(a) (b)

Figure 6: (a) ITG growth rate γ over magnetic shear s without E_r. (b) The ITG growth rate γ versus ω_s with $s = -0.13, 0.6, 0.8$ shown in Fig. 5b, respectively.

With the understanding of magnetic shear tilting effect on ITG mode, the synergistic effect of E_r shear and magnetic shear is investigated. We scan the ITG linear growth rate γ versus ω_s under different magnetic shear, which is shown in Fig. 6b. Under the higher magnetic shear ($s = 0.6, 0.8$), the shearing rate corresponds to the maximum linear growth rate is $\omega_s/\gamma_0 \approx 0.05$, which is smaller than the one ($\omega_s/\gamma_0 \approx 0.10$) that under the weakly reverse magnetic shear ($s = -0.13$). Moreover, the E_r with negative ω_s is more effective in stabilizing ITG under the weakly reverse magnetic shear ($s = -0.13$) compared to the higher magnetic shear. That is because the tilting effect caused by the higher magnetic shear ($s = 0.6, 0.8$) is weak and the ballooning is $\theta_0 \approx 0$, which is shown in Fig. 7c. As a result, the E_r shear become dominant in tilting the ITG mode. From Fig. 6b, the peak value of linear growth rate with normal positive magnetic

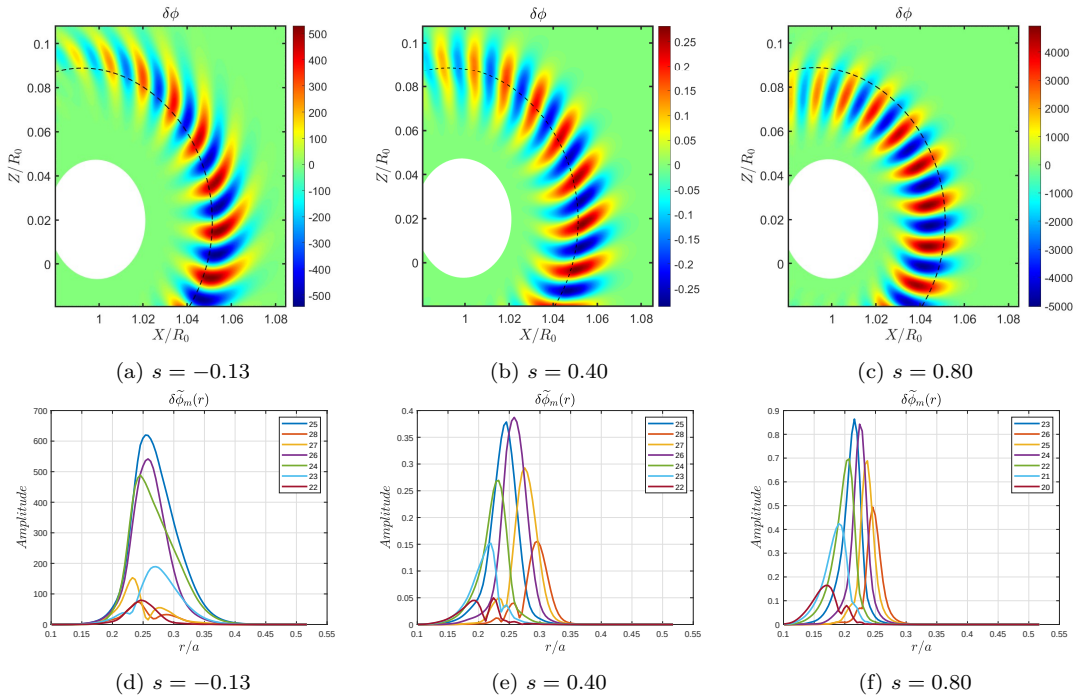

(a) $s = -0.13$ (b) $s = 0.40$ (c) $s = 0.80$

(d) $s = -0.13$ (e) $s = 0.40$ (f) $s = 0.80$

Figure 7: (a)-(c) show the poloidal mode structure of the real part of electrostatic potential with magnetic shear $s = -0.13, 0.40, 0.80$ shown in Fig. 5b, respectively. (d)-(f) show the radial mode profile of different poloidal mode numbers m corresponding the mode structures in top panels.

shear ($s = 0.6, 0.8$) is obviously higher than case with weakly negative magnetic shear ($s = -0.13$). These indicate that it is important to optimize the magnetic shear and the E_r shear simultaneously in order to maximize the stabilizing effect of the E_r shear.

4. Simulation with experimental E_r on EAST

We use the parameters based on a ITB formed case at $5000ms$ on EAST [13] to calculated experimental E_r profile from the radial force balance equation:

$$\partial\phi_{\rm eq}/\partial\psi = -\frac{1}{n_i Z_i}\partial P_i/\partial\psi + q\Omega_\theta - \Omega_\phi \tag{1}$$

where n_i and P_i are the ion density and pressure, q is the safety factor, Ω_θ is the poloidal rotation, ψ is the poloidal flux. However, we focus on the experiments with a weak torque so that the ion pressure gradient is the dominant term in the radial force balance equation and the effects of rotation terms can be ignored [13]. Based on the radial electric field of the experimental configuration as shown in Fig. 8a, we carry out the linear simulation test and find that the ITG mode can be fully stabilized. To better understand the performance of ITG mode under the experimental E_r profile, we consider the amplitude of the E_r and the $\omega_s = 0$ location of the E_r. Because the ITG module structure has a small radial scale, there may be no shearing effect on ITG at the position where $\omega_s = 0$.

Firstly, by multiplying the E_r profile by a coefficient, we change the amplitude of

the E_r profile. The simulation results are shown in Fig. 8b, where the maximum value of the shearing rate ω_s^{max} is used to measure the amplitude of the E_r profile.

The linear growth rate decreases more obviously under the experimental E_r profile, indicating that the E_r well is more efficient than the E_r with constant ω_s on stabilizing the ITG mode.

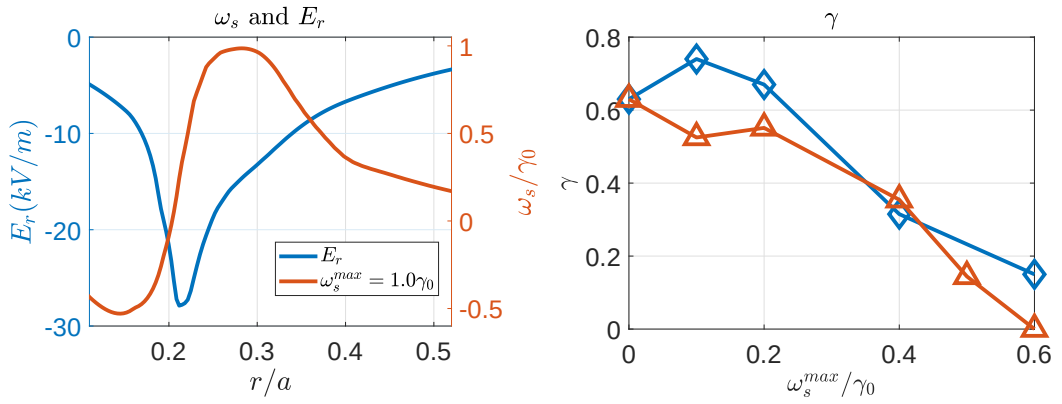

(a) (b)

Figure 8: (a) Left y axis is the experimental E_r directly calculated by the radial force balance equation and the right y is the corresponding shearing rate. (b) The blue line represents the ITG growth rate versus ω_s^{max} for E_r profile with different constant ω_s. The red line denotes the ITG growth rate versus ω_s^{max} for different amplitude of experimental E_r profile with $\omega_s = 0$ at $r/a = 0.20$ as shown in Fig. 8a.

Secondly, the different locations of $\omega_s = 0$ are studied. The $\omega_s = 0$ location at $r/a = 0.20, 0.25, 0.30$ are studied, where $r/a = 0.25$ is the location of ITG. $r/a = 0.20$ and $r/a = 0.30$ denote the $\omega_s = 0$ surface located at the left hand and right hand of the ITG mode, respectively. The E_r profile with different $\omega_s = 0$ location is created by shifted original E_r profile in radial space. We scan $\omega_s^{max}/\gamma_0 = 0.2, 0.4, 0.6$ for each $\omega_s = 0$ setting. The simulation results are shown in Fig. 9a. In comparison with the results with $\omega_s = 0$ location at $r/a = 0.20$ (at the left hand side of the mode), when $\omega_s = 0$ location at $r/a = 0.30$ (at the right hand side of the mode), for $\omega_s^{max}/\gamma_0 = 0.2, 0.4, 0.6$, the ITG mode at the $q = 1$ is fully stabilized, showing that the E_r stabilizing effect is more effective because of the E_r with negative ω_s at the ITG mode location. This result matches the physical mechanism discussed above that the negative ω_s shear is more effective than positive ω_s shear in stabilizing the ITG mode under the weakly reversed magnetic shear. In comparison with the results with $\omega_s = 0$ location at $r/a = 0.20$, when $\omega_s = 0$ location at $r/a = 0.25$ (the mode location), the linear growth rate does not decrease significantly, showing that stabilizing effect caused by E_r shear is noneffective.

Considering the weak effect of E_r for the condition that $\omega_s = 0$ at $r/a = 0.25$, we made simulations for $\omega_s^{max}/\gamma_0 = 0.0, 0.1, 0.2, 0.4, 0.6, 1.2$ in this case. The results are shown in Fig. 9b. The linear growth rates of the ITG mode with $\omega_s^{max}/\gamma_0 = 0.1, 0.2$ are larger than γ_0, which are similar to the result under constant ω_s. However, when the ω_s^{max}/γ_0 increases to $0.6, 1.2$, the linear growth rate of the ITG mode not obviously decreases. The physics discussed in Section 3 can be used to explain the results in

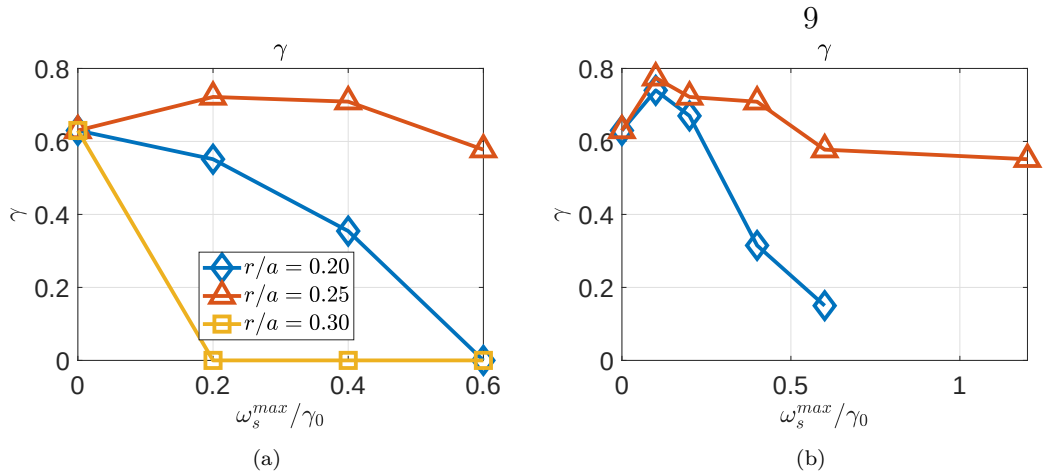

Figure 9: (a) The scanning results of setting $\omega_s = 0$ at different radial location. Notice that the $r/a = 0.20, 0.25, 0.30$ in legend means $\omega_s = 0$ is located at $r/a = 0.20, 0.25, 0.30$. (b) The blue line represents the ITG growth rate versus ω_s^{max} for E_r with different constant ω_s. The rad line denotes the ITG growth rate versus ω_s^{max} for different amplitude of experimental E_r with $\omega_s = 0$ at $r/a = 0.25$.

Fig. 9b. When E_r amplitude gets bigger, the ω_s at the mode location $r/a = 0.25$ is zero, but the ω_s beside the $r/a = 0.25$ gets bigger, which reduces the wavelength of the ITG mode [2]. The small wavelength causes the ITG mode to be locally limited near the $r/a = 0.25$, where has almost zero shearing rate, leading to weakly tilting effect of the ITG mode and no decreasing in the growth rate, which is shown in Fig. 10a–10c. The above results show that the local bottom of the E_r well is the most unfavorable region for stabilizing the ITG mode.

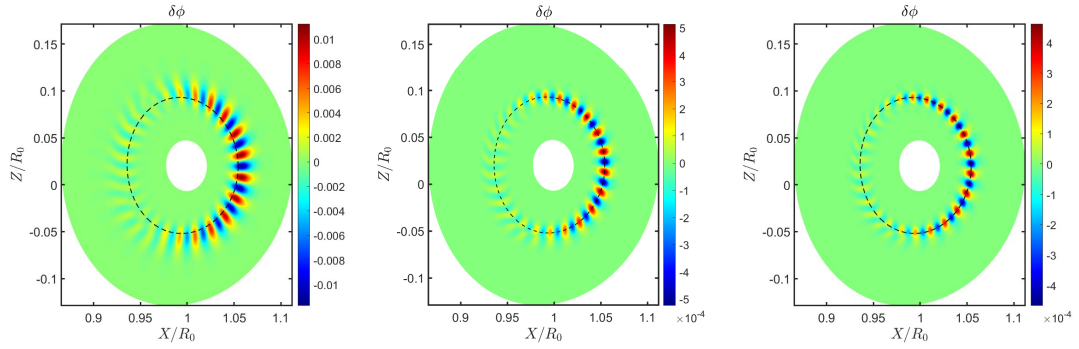

(a) $\omega_s^{max}/\gamma_0 = 0.2$ (b) $\omega_s^{max}/\gamma_0 = 0.6$ (c) $\omega_s^{max}/\gamma_0 = 1.2$

Figure 10: The poloidal mode structure of the real part of electrostatic potential with experimental E_r which $\omega_s = 0$ at $r/a = 0.25$. The $\omega_s^{max}/\gamma_0 = 0.2, 0.6, 1.2$, respectively, and the dashed line indicates the largest η_i and $q = 1$ positions.

Simulation results based on the experimental E_r profile show that the global effect of E_r should be considered even for the micro-instabilities such as ITG instability mode. The local bottom of E_r well has a negative impact on stabilizing the ITG instability mode. In the experiment, in the plasma core, the ion temperature and density increase with the formation of ITB [17], which means an increased ion pressure gradient. The

increasing ion pressure gradient raises the amplitude of the E_r, whose tilting effect will become dominant compared with the weakly reverse magnetic shear and lead the net effect stabilizes the ITG mode and reduces the turbulence transport. Besides, the experiment research [18] showed that the E_r well bottom will shift outward in radial direction, which matches our results that the E_r with $\omega_s = 0$ location at $r/a = 0.30$ has more efficient stabilizing effect on ITG mode because of the synergistic effect between the negative ω_s and the weakly reverse magnetic shear. Therefore, it is very likely that there is a mechanism of positive feedback between the formation of the ITB and the formation of the E_r, leading to an increase in the E_r amplitude and the outward movement of ω_s location combined with the reversed magnetic shear, which might be the key to the formation and the long-time existence of ITB. Moreover, in order to reduce the transport by ITG, it is better to control the E_r with negative ω_s in the reversed magnetic shear region, e.g. using NBI which can induce plasma rotation to affect the E_r profile [19].

5. Conclusion

Based on EAST configuration, the synergistic effect of the E_r shear and magnetic shear on turbulence is studied by GTC. In contrast to the previous stabilizing effect of the E_r shear on ITG, it is found that whether the E_r shear is stabilizing or destabilizing not only depends on the amplitude of the E_r shear, but also on the relative direction between the E_r shear and the magnetic shear. Under the weakly reversed magnetic shear, E_r shear is destabilizing for small positive shearing rate, while it is stabilizing when positive shearing rate is large enough. For negative shearing rate, E_r shear always plays a stable role, and is more efficient than that with positive shearing rate. Because the negative ω_s shear and the weakly magnetic shear have the same mode tilting direction. The simulation results also indicate that the ITG mode is more unstable under the positive magnetic shear.

The global effect of E_r profile should be considered in stabilizing ITG instability for experimental E_r. The E_r with the $\omega_s = 0$ at the right side of the ITG mode shows a better stabilizing effect compared with the $\omega_s = 0$ at the left side, because of the synergistic effect of the negative ω_s and the weakly reverse magnetic shear at the ITG mode location. The positive feedback between the formation of the ITB and the formation of the E_r will increase the E_r amplitude and cause the outward movement of the ω_s location combined with the reversed magnetic shear, which might be the key to the formation and the long-time existence of ITB. Moreover, Neutral Beam Injection is expected to manipulate the E_r profile with negative ω_s in the reversed magnetic shear region, which will stabilize ITG mode and reduce the transport by ITG mode. The nonlinear simulations will be carried out in future, which might further illustrate the synergistic effect on the ITG induced transport.

Acknowledge

This work is supported by the National Key R&D Program of China (Grant Nos. 2024YFE03001102), the Strategic Priority Research Program of Chinese Academy of Sciences (Grant Nos. XDB0790202 and XDB0500302). The numerical calculations in this paper were performed on the Hefei Advanced Computing Center.

References

[1] J.W. Connor, T. Fukuda, X. Garbet, C. Gormezano, V. Mukhovatov, M. Wakatani, the ITB Database Group, the ITPA Topical Group on Transport, and Internal Barrier Physics. A review of internal transport barrier physics for steady-state operation of tokamaks. *Nuclear Fusion*, 44(4):R1, March 2004.

[2] K. H. Burrell. Effects of E×B velocity shear and magnetic shear on turbulence and transport in magnetic confinement devices. *Physics of Plasmas*, 4(5):1499–1518, May 1997.

[3] Jr. Antonsen, T. M., J. F. Drake, P. N. Guzdar, A. B. Hassam, Y. T. Lau, C. S. Liu, and S. V. Novakovskii. Physical mechanism of enhanced stability from negative shear in tokamaks: Implications for edge transport and the L-H transition. *Physics of Plasmas*, 3(6):2221–2223, June 1996.

[4] S. Taimourzadeh, L. Shi, Z. Lin, R. Nazikian, I. Holod, and D. Spong. Effects of rmp-induced changes of radial electric fields on microturbulence in diii-d pedestal top. *Nuclear Fusion*, 59(4):046005, February 2019.

[5] Y C Chen, Y Q Qin, G Y Sun, and Z Lin. The performance of equilibrium radial electric field shear on microturbulence with different magnetic shears in tokamak plasmas. *Plasma Physics and Controlled Fusion*, 65(7):075005, May 2023.

[6] W H Wang, J Bao, X S Wei, Z Lin, G J Choi, S Dettrick, A Kuley, C Lau, P F Liu, and T Tajima. Effects of equilibrium radial electric field on ion temperature gradient instability in the scrape-off layer of a field-reversed configuration. *Plasma Physics and Controlled Fusion*, 63(6):065001, April 2021.

[7] J. Y. Fu, J. H. Nicolau, P. F. Liu, X. S. Wei, Y. Xiao, and Z. Lin. Global gyrokinetic simulation of neoclassical ambipolar electric field and its effects on microturbulence in W7-X stellarator. *Physics of Plasmas*, 28(6):062309, June 2021.

[8] T J J Tala, J A Heikkinen, V V Parail, Yu F Baranov, and S J Karttunen. Itb formation in terms of e×b flow shear and magnetic shear s on jet. *Plasma Physics and Controlled Fusion*, 43(4):507, April 2001.

[9] R. E. Waltz, G. M. Staebler, W. Dorland, G. W. Hammett, M. Kotschenreuther, and J. A. Konings. A gyro-landau-fluid transport model. *Physics of Plasmas*, 4(7):2482–2496, 07 1997.

[10] Z Lin, Y Nishimura, Y Xiao, I Holod, W L Zhang, and L Chen. Global gyrokinetic particle simulations with kinetic electrons. *Plasma Physics and Controlled Fusion*, 49(12B):B163, November 2007.

[11] Yuehao Ma, Bin Zhang, Jian Bao, Z. Lin, Wenlu Zhang, Huishan Cai, and Ding Li. Electrostatic turbulence in east plasmas with internal transport barrier. *Nuclear Fusion*, 63(5):056014, March 2023.

[12] J Citrin, H Arnichand, J Bernardo, C Bourdelle, X Garbet, F Jenko, S Hacquin, M J Pueschel, and R Sabot. Comparison between measured and predicted turbulence frequency spectra in itg and tem regimes. *Plasma Physics and Controlled Fusion*, 59(6):064010, May 2017.

[13] B. Zhang, X. Gong, J. Qian, L. Zeng, L.Q. Xu, Y.M. Duan, J.Y. Zhang, Y.C. Hu, T.Q. Jia, P. Li, R.R. Liang, Z.H. Wang, X. Zhu, S.X. Wang, Q. Ma, L. Ye, J. Huang, R. Ding, and the EAST Team. Progress on physics understanding of improved confinement with fishbone

instability at low q95 < 3.5 operation regime in east. *Nuclear Fusion*, 62(12):126064, November 2022.

[14] R. L. Miller, F. L. Waelbroeck, A. B. Hassam, and R. E. Waltz. Stabilization of ballooning modes with sheared toroidal rotation. *Physics of Plasmas*, 2(10):3676–3684, 10 1995.

[15] Y. Kishimoto, J.-Y. Kim, W. Horton, T. Tajima, M.J. LeBrun, S.A. Dettrick, J.Q. Li, and S. Shirai. Discontinuity model for internal transport barrier formation in reversed magnetic shear plasmas. *Nuclear Fusion*, 40(3Y):667, March 2000.

[16] J. Zielinski, M. Becoulet, A. I. Smolyakov, X. Garbet, G. T. A. Huijsmans, P. Beyer, and S. Benkadda. Global ITG eigenmodes: From ballooning angle and radial shift to Reynolds stress and nonlinear saturation. *Physics of Plasmas*, 27(7):072507, July 2020.

[17] K Ida and T Fujita. Internal transport barrier in tokamak and helical plasmas. *Plasma Physics and Controlled Fusion*, 60(3):033001, jan 2018.

[18] X. Q. Wu T. Zhang B. Lyu X. Gao D. Jiang, Y. Y. Li and G. S. Xu. Edge toroidal rotation analysis by cxrs diagnostic on east. *Fusion Science and Technology*, 76(6):723–730, 2020.

[19] Xingyuan Xu, Yingfeng Xu, Xiaodong Zhang, and Youjun Hu. Simulations of the radial electric field induced by neutral beam injection in a tokamak. *Nuclear Fusion*, 61(8):086002, jun 2021.